

# Integrated transcriptome and trajectory analysis of cutaneous T-cell lymphoma identifies putative precancer populations

Jingjing Ren,<sup>1,\*</sup> Rihao Qu,<sup>2,3,\*</sup> Nur-Taz Rahman,<sup>4,\*</sup> Julia M. Lewis,<sup>1</sup> Amber Loren Ong King,<sup>1</sup> Xiaofeng Liao,<sup>5</sup> Fatima N. Mirza,<sup>1</sup> Kacie R. Carlson,<sup>1</sup> Yaqing Huang,<sup>3</sup> Scott Gigante,<sup>6</sup> Benjamin Evans,<sup>7</sup> Barani Kumar Rajendran,<sup>5</sup> Suzanne Xu,<sup>1</sup> Guilin Wang,<sup>8</sup> Francine M. Foss,<sup>9</sup> William Damsky,<sup>1,3</sup> Yuval Kluger,<sup>3</sup> Smita Krishnaswamy,<sup>10</sup> and Michael Girardi<sup>1</sup>

<sup>1</sup>Department of Dermatology, <sup>2</sup>Department of Immunobiology, <sup>3</sup>Department of Pathology, <sup>4</sup>Bioinformatics Support Program, Cushing/Whitney Medical Library, and <sup>5</sup>Department of Pharmacology, Yale School of Medicine, New Haven, CT; <sup>6</sup>Computational Biology and Bioinformatics Program and <sup>7</sup>Yale Center for Research Computing, Yale University, New Haven, CT; <sup>8</sup>Yale Center for Genome Analysis and <sup>9</sup>Section of Medical Oncology, Department of Internal Medicine, Yale School of Medicine, New Haven, CT; and <sup>10</sup>Department of Genetics, Yale University, New Haven, CT

## Key Points

- Integrated transcriptome analyses identify putative precancerous circulating clonal CD4<sup>+</sup> T-cell populations in patients with CTCL.
- The study results reveal promising therapeutic strategies via targeting of CD82 and JAK kinases.

The incidence of cutaneous T-cell lymphoma (CTCL) increases with age, and blood involvement portends a worse prognosis. To advance our understanding of the development of CTCL and identify potential therapeutic targets, we performed integrative analyses of paired single-cell RNA and T-cell receptor (TCR) sequencing of peripheral blood CD4<sup>+</sup> T cells from patients with CTCL to reveal disease-unifying features. The malignant CD4<sup>+</sup> T cells of CTCL showed highly diverse transcriptomic profiles across patients, with most displaying a mature Th2 differentiation and T-cell exhaustion phenotype. TCR-CDR3 peptide prediction analysis suggested limited diversity between CTCL samples, consistent with a role for a common antigenic stimulus. Potential of heat diffusion for affinity-based trajectory embedding transition analysis identified putative precancerous circulating populations characterized by an intermediate stage of gene expression and mutation level between the normal CD4<sup>+</sup> T cells and malignant CTCL cells. We further revealed the therapeutic potential of targeting CD82 and JAK that endow the malignant CTCL cells with survival and proliferation advantages.

## Introduction

Cutaneous T-cell lymphoma (CTCL) is a heterogeneous group of non-Hodgkin lymphomas.<sup>1</sup> The most common form of CTCL exists on a spectrum of mycosis fungoides (MF) and Sézary syndrome (SS), characterized by malignant clones of skin-homing CD4<sup>+</sup> T cells that may expand in the peripheral blood of patients with advanced disease and are indicative of a worse prognosis. The advanced forms of MF and SS CTCLs are more likely to show blood involvement and include patients with erythrodermic stage III disease, with a median survival rate of 4 to 6 years, and extracutaneous disease stage IVA (lymph nodes) or IVB (viscera), with a survival of <1.5 years.<sup>2</sup> Analyses by comparative genomic hybridization<sup>3,4</sup> and exome and whole-genome sequencing<sup>5-10</sup> have revealed marked genetic heterogeneity across malignant cells of patients with CTCL, in particular within somatic copy number variations (SCNVs) relative to other cancers, but also within somatic single-nucleotide variations (SSNVs). Despite this

Submitted 23 May 2022; accepted 20 July 2022; prepublished online on *Blood Advances* First Edition 10 August 2022. <https://doi.org/10.1182/bloodadvances.2022008168>.

\*J.R., R.Q., and N.-T.R. contributed equally to this study.

The scRNAseq data reported in this article have been deposited in the Gene Expression Omnibus database (accession number GSE197619).

All scripts for bioinformatic analysis are available upon request from the corresponding author, Michael Girardi ([michael.girardi@yale.edu](mailto:michael.girardi@yale.edu)).

The full-text version of this article contains a data supplement.

© 2023 by The American Society of Hematology. Licensed under [Creative Commons Attribution-NonCommercial-NoDerivatives 4.0 International \(CC BY-NC-ND 4.0\)](https://creativecommons.org/licenses/by-nc-nd/4.0/), permitting only noncommercial, nonderivative use with attribution. All other rights reserved.

mutational diversity, transcriptome profiling<sup>5,11-13</sup> has shown that CTCL cells have high expression of several genes and their products, including *TOX*, *TPO*, *PLS3*, *KIR3DL2*, *CCR4*, and *GATA3*, 2 of which are targets of the current anti-CCR4 (mogamulizumab) and anti-KIR3DL2 (lacutamab) monoclonal antibody therapies. Somatic mutations in genes encoding T-cell receptors (TCRs) and JAK-STAT molecules have also been characterized in CTCL, including SSNVs of *JAK1*, *JAK2*, and *JAK3*, and SCNV amplifications of *STAT3* and *STAT5B*, and aberrant *JAK3/STAT* signaling has been identified as a mechanism that promotes proliferation and survival of CTCL cells.<sup>7,14-16</sup> However, ex vivo studies<sup>17,18</sup> have revealed that JAK inhibition via nonspecific JAK targeting is variably effective at limiting CTCL survival, raising the question of whether more specific kinase inhibitors may be more effective.

Although the etiology and pathogenesis of CTCL have yet to be fully elucidated, a proposed<sup>19</sup> progression includes a combination of chronic TCR stimulation and survival-enhancing mutations induced by inherited factors and/or environmental exposures of mature peripheral skin-homing CD4<sup>+</sup> T cells. Examples include cutaneous or systemic chemical exposures<sup>20</sup> and UV radiation,<sup>5,7</sup> telomeric-shortening-associated chromosomal instability,<sup>21,22</sup> SCNV selection, and accumulation of SSNV mutations that, in concert, drive the antiapoptotic, proliferative, chronic T-cell activating, and antitumor immune inhibiting behavior of CTCL cells. In fact, UV signature mutations have contributed to the mutational burden in 52% of patients with MF and 23% of patients with SS.<sup>23,24</sup>

Although these specific genetic and transcriptomic features of CTCL cells have been identified, the most widely used strategies for assessing malignant hematological involvement in patients with CTCL rely on immunophenotypic identification of CTCL cells as CD4<sup>+</sup> CD26<sup>-</sup> and/or CD4<sup>+</sup>CD7<sup>-</sup> or by expansion of the TCRVβ family.<sup>25</sup> However, these immunophenotypes may have substantial overlap with nonmalignant CD4<sup>+</sup> T cells. Alternatively, mRNA sequencing of the completely rearranged TCRαβ heterodimer may be used as part of a multiomics approach to characterize more precisely the malignant T-cell clone relative to other CD4<sup>+</sup> T cells while potentially identifying any other T-cell populations<sup>26,27</sup> that may share the TCR clonotype with the bona fide CTCL cells. One such population may be precancerous or intermediate cells (ie, those that comprise a group of premalignant cells that are intermediate in the transition from normal to malignant cells and that are capable of increasing the risk of cancer development and subsequently may coexist with the malignant cells with the potential to influence tumor burden<sup>28,29</sup>).

In our study, we paired single-cell RNA sequencing (scRNAseq) with TCRαβ sequencing (scTCRseq) of CD4<sup>+</sup> T cells from 11 patients with CTCL with documented blood involvement and 3 healthy volunteers, to better characterize malignant T cells compared with non-CTCL CD4<sup>+</sup> cells within patients and with normal CD4<sup>+</sup> T cells from healthy controls. By performing individual patient scRNAseq analysis along with the potential of heat diffusion for affinity-based trajectory embedding (PHATE) analysis<sup>30</sup> in combination with scTCRseq and CTCL clonotyping, we constructed the trajectory of cells along with the transition from normal CD4<sup>+</sup> T cells to bona fide CTCL cells and identified putative precancerous cells that were consistently intermediate in the expression of CTCL-defining genes and inferred mutation load. We extended these findings by exploring the therapeutic potential of a CTCL cell-overexpressing gene, *CD82*, which belongs to the

tetraspanin family and has also been reported to promote the proliferation of acute myelogenous leukemia (AML) cells via *STAT5A* and *AKT* signaling.<sup>31-33</sup> However, the role of *CD82* in CTCL pathogenesis is unknown. In prior studies we found that patient-derived CTCL cells exhibit variable sensitivity to the JAK inhibitor ruxolitinib, and we now show that CTCL cells rendered *CD82* deficient are specifically associated with phospho-JAK/STAT downregulation. Thus, our investigation also compared the relative potential of a spectrum of JAK inhibitors in treatment of CTCL. These integrated transcriptomic and trajectory analyses collectively provide fundamental insights into the development and progression of and potential therapeutics for CTCL.

## Methods

### Patient samples

Peripheral blood from patients with CTCL and healthy donors was collected in lithium heparin tubes at the Yale Cancer Center after obtaining written informed consent and following all regulations in accordance with the Yale Human Investigational Review Board. Procedures for isolation of various cell populations, cell culture, JAK inhibitor screening, and flow cytometry are described within the supplemental Methods.

### scRNA library preparation and sequencing

Libraries were prepared by the Yale Center for Genome Analysis using single-cell library preparation kits from 10x Genomics. Single-cell library kits, RNA data processing, quality control, and analysis methods are presented in the supplemental Methods.

### SSNV and SCNV analyses

CellSNP mode 1<sup>34</sup> was leveraged to infer SSNV per cell for all samples. The R package InferCNV<sup>35</sup> was used to infer SCNV at a single-cell level. Both are further described in the supplemental Methods.

### CD82 knockout via CRISPR-Cas9

Purified malignant T cells from the peripheral blood of patients were cultured for 3 days, and *CD82* gene knockout was performed according to the Integrated DNA Technologies protocol, as described in the supplemental Methods.

## Results

### Integrative analysis of paired mRNA single-cell transcriptome and TCR sequencing of CD4<sup>+</sup> T cells from patients with CTCL reveals the heterogeneity of CTCLs

Purified CD4<sup>+</sup> T cells from the peripheral blood of 11 patients with CTCL (Table 1) and 3 healthy individuals were analyzed by 5' scRNAseq and paired scTCRseq (Figure 1A). We found that the dominant TCR clone in each patient with CTCL was substantially expanded, reflecting their CTCL identification by both scRNAseq data analysis and TCR clonal identity (Figure 1B). To identify common features among CTCL cells from disparate patients, we performed a Seurat integration analysis (Figure 1C). Unsupervised clustering of cells was represented by 2-dimensional Uniform Manifold Approximation and Projection, followed by the annotation

**Table 1. Patient information**

Sample ID	Age	Sex	ISCL stage	B stage	CTCL subtype	Clinically abnormal phenotype	% CD4 <sup>+</sup> CD26 <sup>-</sup>	Abs. abn. <sup>a</sup> (/μL)	Treatment
P1	81	M	IVA	B2	SS	CD3dim <sup>+</sup> CD4 <sup>+</sup> CD7 <sup>-</sup> CD26 <sup>-</sup> CD2 <sup>+</sup> CD8 <sup>-</sup> CD10 <sup>-</sup> CD5 <sup>+</sup>	87.8	1818.3	ECP, ACIT
P2	76	M	IIB	B1	MF	CD3dim <sup>+</sup> CD4 <sup>+</sup> CD7 <sup>-</sup> CD26 <sup>-</sup> CD8 <sup>-</sup> CD5 <sup>+</sup> CD2 <sup>+</sup>	37.4	1774.6	ECP, BEX
P3	72	F	IVA	B2	SS	CD3 <sup>+</sup> CD4 <sup>+</sup> CD7Var <sup>+</sup> CD26 <sup>-</sup> CD8 <sup>-</sup> CD2 <sup>+</sup> CD25 <sup>-</sup>	82.6	2799.6	ECP, BEX, IFN-α
P4	79	M	IA	B1	MF	CD3dim <sup>+</sup> CD4 <sup>+</sup> CD7 <sup>-</sup> CD26 <sup>-</sup> CD2 <sup>+</sup>	61.2	964.5	ECP, BEX
P5	56	M	IVA	B2	SS	CD3 <sup>+</sup> CD4 <sup>+</sup> CD7 <sup>+</sup> CD26 <sup>-</sup> CD2dim <sup>+</sup> CD8 <sup>-</sup> CD5 <sup>+</sup> CD25 <sup>-</sup>	60.1	973.6	ECP, BEX
P6	85	M	IVA	B2	SS	CD3 <sup>+</sup> CD4 <sup>+</sup> CD7dim <sup>-</sup> CD26 <sup>-</sup> CD2Var <sup>+</sup> CD8 <sup>-</sup> CD5 <sup>+</sup>	74.1	1387.2	ECP, BEX
P7	78	F	IVA	B2	SS	CD3 <sup>+</sup> CD4 <sup>+</sup> CD7 <sup>-</sup> CD26 <sup>-</sup> CD5 <sup>+</sup> CD8 <sup>-</sup>	42.3	802.0	ECP, BEX, VRS
P8	74	F	IVA	B2	SS	CD3 <sup>+</sup> CD4 <sup>+</sup> CD7 <sup>+</sup> CD26 <sup>-</sup> CD8 <sup>-</sup>	89.0	979.0	Moga
P9	68	F	IVA	B1	SS	CD3dim <sup>+</sup> CD4dim <sup>+</sup> CD7 <sup>-</sup> CD26dim <sup>-</sup> CD2dim <sup>+</sup> CD8 <sup>-</sup> CD10 <sup>-</sup> CD5dim <sup>+</sup> CD25 <sup>-</sup>	51.9	356.2	ECP, BEX, IFN-α, IFN-γ
P10	70	M	IIB	B1	MF	CD3 <sup>+</sup> CD4 <sup>+</sup> CD7 <sup>-/+</sup> CD26 <sup>-</sup> CD5dim <sup>+</sup>	44.8	503.9	ECP, BEX
P11	76	M	IIB	B1	MF	CD3dim <sup>+</sup> CD4dim <sup>+</sup> CD7 <sup>-</sup> CD26 <sup>-</sup> CD5 <sup>+</sup>	58.0	580.0	ECP, BEX, IFN-α

ISCL stage and B stage are at diagnosis, and blood counts and treatments are at the time of sequencing. Abs. abn., absolute numbers of abnormal cells; ACIT, acitretin; BEX, bexarotene; ECP, extracorporeal photopheresis; IFN-α, interferon-α; ISCL, International Society for Cutaneous Lymphomas; Lymph, lymphocytes; Moga, mogamulizumab; VRS, Vorinostat; WBC, white blood cell. <sup>a</sup>Abs. abn. = (% CD4<sup>+</sup>CD26<sup>-</sup> × % lymph.)/10 000 × WBC × 1000.

of CTCL cells and normal CD4<sup>+</sup> T cells of each patient based on the dominant CDR3 TCR sequence (Figure 1D). Integration revealed that normal CD4<sup>+</sup> T cells from different patients co-clustered, whereas the CTCL cells of individual patients each clustered separately, distinguished from each other and from the unified normal CD4<sup>+</sup> T-cell cluster (Figure 1C).

When we selectively included only annotated CTCL cells for clustering analysis, individual patients' cells clustered distinctly. This is also demonstrated by a heat map that shows that each CTCL cluster has a distinguishing gene signature (supplemental Figure 1). Furthermore, annotation of CTCLs by T-helper (Th) cell subset hallmark genes (Th2-like: *GATA3* >1, *CCR4* >1; T-regulatory (Treg)-like: *FOXP3* >1, *CTLA4* >1; T-follicular helper (Tfh)-like: *PDCD1* >1, *CXCR5* >1; and Th17-like: *RORC* >1, *CCR6* >1) also revealed the diversity of CTCL cells among different patients, but with a Th2-like phenotype more than the Treg-, Tfh-, or Th17-like phenotype. In contrast, there was little to no Th1-like differentiation among the CTCL cells (Figure 1E). In 10 of the 11 CTCL patient samples, TCR clonotype profiling of the CTCL cluster in each patient showed a single dominant TCR clone (the exception being patient 6 [P6], where 2 TCRα and 2 TCRβ sequences were present within each CTCL cell), confirming that CTCLs are monoclonally expanded. Taken together, our data demonstrated wide transcriptomic and TCR clonotypic heterogeneity among patients with CTCL, albeit with features of a Th2 differentiation propensity.

**PHATE analysis reveals putative precancerous intermediate CD4<sup>+</sup> T-cell populations in patients with CTCL**

CTCL is believed to be derived from mature effector T cells with increased age-associated risk, suggesting that an accumulation of genetic mutations may play an important role in CTCL development. Given that TCR clonality is a fundamental feature of CTCL, TCR clonal status may provide insight into the history of CTCL developmental. With this understanding, we hypothesized that a group of

genotypically and transcriptionally transitory circulating CD4<sup>+</sup> T cells (ie, intermediate in transitioning from normal CD4<sup>+</sup> T cells to malignant CTCL cells) may be present in patients with CTCL. To test our hypothesis, we performed scRNAseq analysis and CTCL scTCRseq clonal annotation for each patient separately. We consistently observed that total CD4<sup>+</sup> T cells produced 2 general clusters clearly delineated as CTCLs vs normal CD4<sup>+</sup> T cells, (Figure 2A; supplemental Figure 2). However, TCR clonotype annotation (Figure 2B) consistently revealed in each patient an expanded population of normal-clustering CD4<sup>+</sup> T cells that shared the identical TCR clonotype with the malignant CTCL cells. When we sub-clustered the normal T cells, those normal T cells expressing the CTCL TCR clonotype were contained within a new cluster (Figure 2C-D; supplemental Figure 2). When we compared the CTCL clonotype frequency to all-clonotype mean frequency in both the total normal CD4<sup>+</sup> T-cell cluster and the CTCL clonotype-containing subcluster, we found that the CTCL clonotype frequency was significantly higher, indicating a previous level of clonal expansion in the CTCL clonotype-positive, yet normal clustering, CD4<sup>+</sup> T cells (Figure 2E-F).

We next used PHATE analysis, which enables the visualization of high-dimensional data with cell trajectory structure to predict the developmental direction of different cell clusters,<sup>30</sup> and found that the cluster of normal T cells containing the CTCL clonotype was consistently situated between the main population of normal T cells (that is, those without the dominant CTCL-clonotype) and the main CTCL cluster (Figure 2G-H; supplemental Figure 3). This finding further suggests that a putative transitional population exists between normal CD4<sup>+</sup> T cells and established CTCL cells (Figure 2E-F; supplemental Figure 3). Transferring the group identity of cells from the single-patient analysis to a CTCL patient-integrated object also revealed the 3 groups: CTCLs, normal CD4<sup>+</sup> T cells, and intermediate transitional CD4<sup>+</sup> T cells (Figure 3A; top). When differential expression genes (DEGs) were assessed within this integrated dataset, in all cases the transitional CD4<sup>+</sup> T cells had expression that was intermediate between that of normal

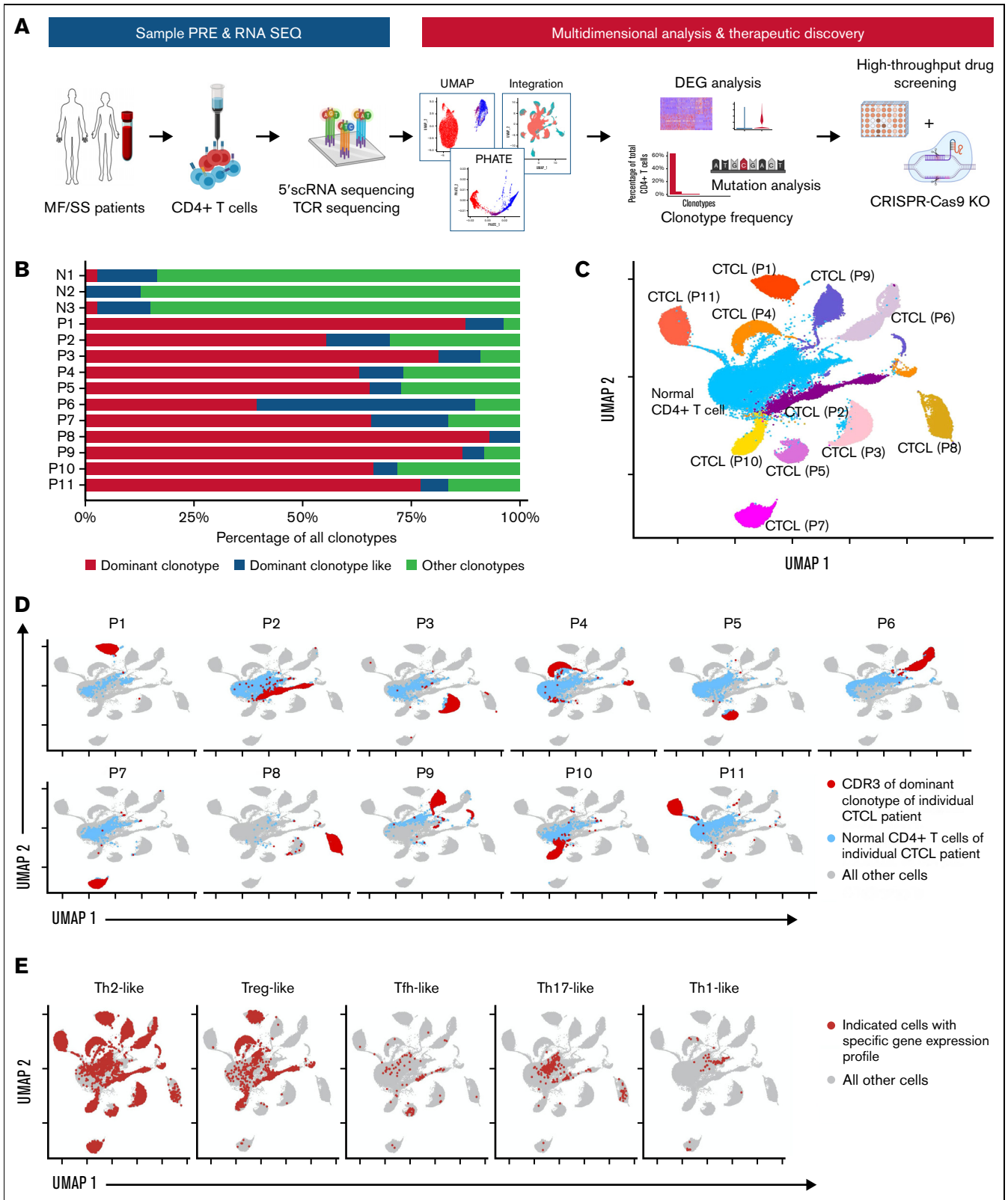


**Figure 1. Characterization of transcriptional heterogeneity between patients with CTCL by paired scRNAseq and sTCRseq analyses of CD4<sup>+</sup> T cells.** CD4<sup>+</sup> T cells purified from the peripheral blood of 11 patients with CTCL underwent paired single-cell mRNA and TCR VDJ sequencing. (A) Summary of study design including sample preparation, sequencing, multidimensional data analysis, and mechanistic studies. (B) TCR clonotype frequency in purified CD4<sup>+</sup> T cells from patients with CTCL (P1-P11) and healthy controls (N1-N3). Dominant clonotype: most frequent complete TCR $\alpha$  and TCR $\beta$  CDR3 transcripts. Dominant clonotype-like: TCR $\alpha$  CDR3 or TCR $\beta$  CDR3 matching the

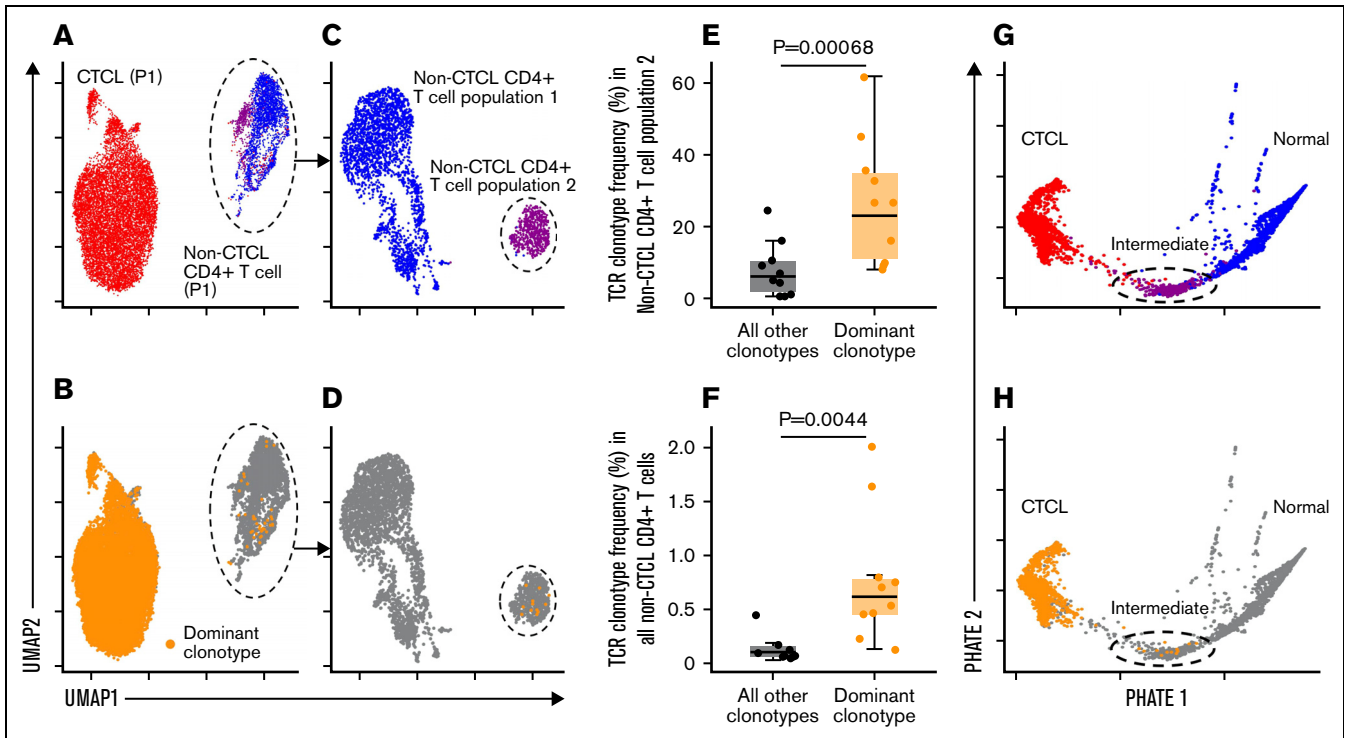


**Figure 2. PHATE analysis reveals circulating putative precancerous intermediate CD4<sup>+</sup> T-cell populations in CTCL.** (A) Representative UMAP plot of CD4<sup>+</sup> T cells from a patient with CTCL resulted in 2 major separate annotated clusters: CTCL cells (red) and non-CTCL CD4<sup>+</sup> T cells (blue+purple). (C) The non-CTCL CD4<sup>+</sup> T cells were further divided into 2 clusters: population 1 (blue), and population 2 (purple). (B,D) The dominant TCR clonotype is highlighted in yellow over the same UMAP. A group of cells containing the dominant clonotype fell within the non-CTCL CD4<sup>+</sup> T-cell population upon unsupervised clustering. A comparison of the mean frequency of the dominant (malignant) TCR clonotype vs all other TCR clonotypes in the non-CTCL CD4<sup>+</sup> T-cell population 2 (E) and in the total non-CTCL CD4<sup>+</sup> T-cell population (F) revealed that the dominant clonotype frequency was overrepresented in both populations ( $n = 10$ , paired  $t$  test). (G) PHATE mapping revealed the non-CTCL CD4<sup>+</sup> T-cell population 2 to be an intermediate group of cells (purple) falling between normal CD4<sup>+</sup> T cells (blue) and CTCL cells (red). (H) This intermediate group contained cells with the dominant clonotype, highlighted in yellow throughout the PHATE map. UMAP, Uniform Manifold Approximation and Projection.

CD4<sup>+</sup> T cells and malignant CTCL cells (Figure 3, bottom; supplemental Figure 4). We also performed analyses to detect SSNVs<sup>34</sup> and SCNVs<sup>35</sup> inferred from the scRNAseq data (Figure 3B-E). Once again, our putative transitional CD4<sup>+</sup> populations suggested a premalignant state with mutation levels intermediate between normal CD4<sup>+</sup> T cells and the CTCL cells, notably with mutational diversity that was limited to a smaller subset of that found within each CTCL population's SSNVs (Figure 3B). Similarly, a subset of CTCL SCNVs was shared with the transitional CD4<sup>+</sup> population (Figure 3E). Projection of SCNV level onto the PHATE map revealed a progressive increase from normal CD4<sup>+</sup> T cells, to transitional cells, to CTCL cells (Figure 3F-G). These findings collectively reveal that, in each patient, there was an expanded clone of T cells, TCR matched to each malignant CTCL cell population, with intermediate levels of expression of

CTCL-defining genes, including those indicative of Th2 differentiation status (supplemental Figure 5), as well as mutational loads, suggesting that such intermediate cells represent precancerous populations involved in development of CTCL.

### Integrative analysis identifies common DEGs and fundamental pathways among heterogeneous CTCL patient samples

Despite the heterogeneity among CTCL patient samples, we looked for common features of CTCL by integrative analysis. DEG analysis was performed to compare all CTCL cells to total normal CD4<sup>+</sup> T cells from patients and to all CD4<sup>+</sup> T cells from healthy controls. Plotting the Uniform Manifold Approximation and Projection and heat map (Figure 4A) revealed 66 upregulated genes and

**Figure 1 (continued)** top clonotype in the absence of any transcript for the other chain. Other clonotypes: all other TCR $\alpha$  and/or TCR $\beta$  CDR3 transcripts. Note that in P6, 2 complete TCR $\alpha$  and 2 complete TCR $\beta$  sequences were present in the dominant clonotype. (C) A UMAP resulting from the integration of the scRNAseq transcriptomes of samples derived from 11 patients with CTCL (112 840 single cells distributed by annotated, unsupervised clustering) highlights interpatient diversity (each patient with CTCL is distinctly colored), as well as commonality of normal CD4<sup>+</sup> T cells among the different patients (blue). (D) Total CD4<sup>+</sup> T cells from each patient are individually highlighted throughout the integrated UMAP: normal CD4<sup>+</sup> T cells (blue), CTCL cells (highlighted in red according to the dominant CDR3 sequence of each patient). (E) T-cell subsets based on characteristic gene expression are highlighted throughout the integrated UMAP. Th2-like: *GATA3* >1, *CCR4* >1; Treg-like: *FOXP3* >1, *CTLA4* >1; Tfh-like: *PDCD1* >1, *CXCR5* >1; Th17-like: *RORC* >1, *CCR6* >1. (The gene cutoff of 1 indicates that the normalized and scaled gene expression is >1.) UMAP, Uniform Manifold Approximation and Projection.

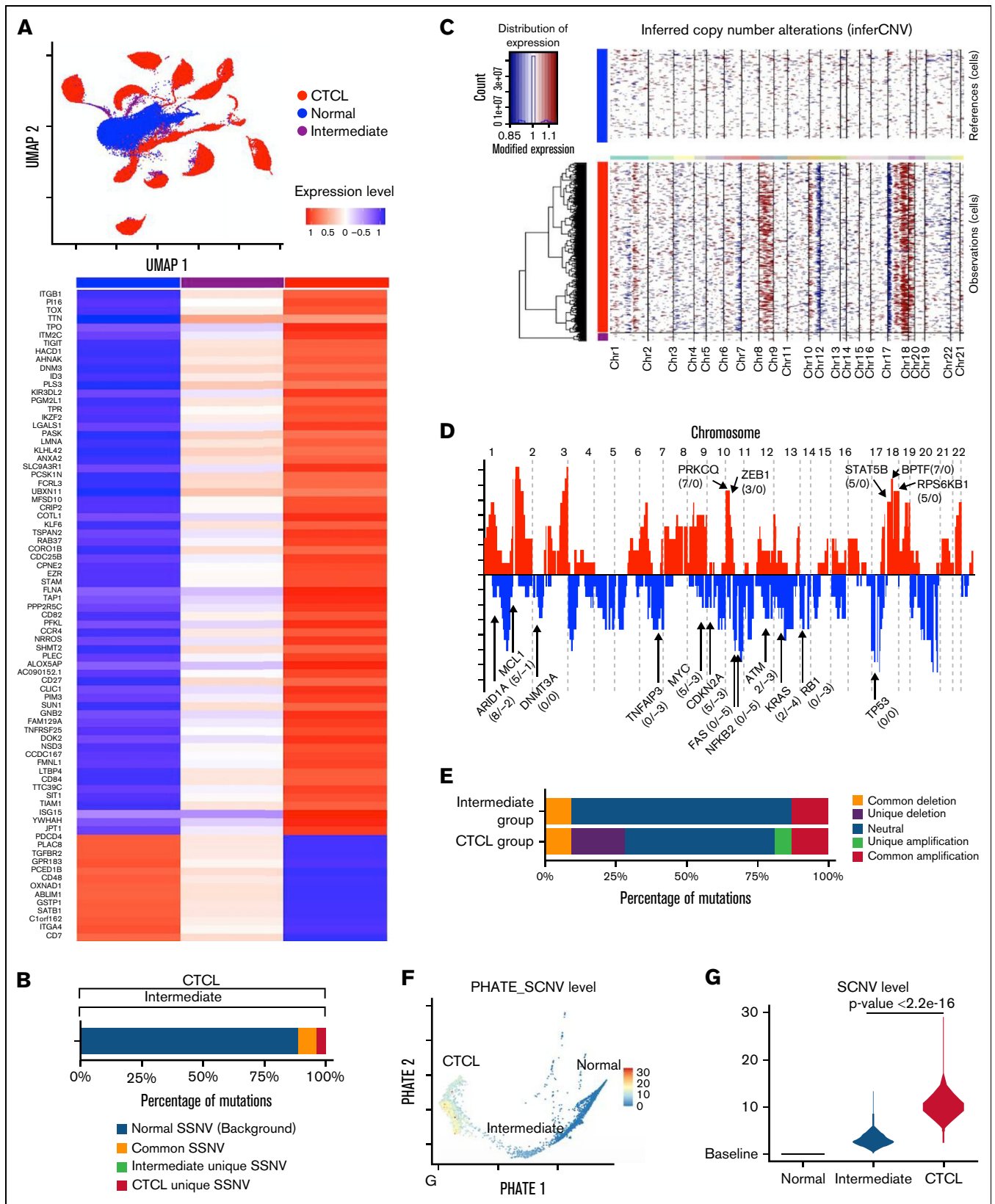


Figure 3.

13 downregulated genes within CTCL cells compared with both normal CD4<sup>+</sup> T-cell populations. Pathway and enrichment analysis by Enrichr<sup>36,37</sup> (<https://maayanlab.cloud/Enrichr/>) using The Molecular Signatures Pathway Database (MsigDB\_Hallmark\_2020) identified 18 significantly (adjusted  $P \leq .05$ ) enriched pathways (supplemental Table 1). Several signaling pathways involved in T-cell activation and downstream of TCR signaling (eg, allograft rejection, reactive oxygen species, tumor necrosis factor, hypoxia, and mTORC-1) were notably enriched in CTCL cells relative to normal CD4<sup>+</sup> T cells (Figure 4B). Despite the fact that our analyses integrated scRNAseq and scTCRseq data, the enrichment pathways of DEGs from previously published bulk RNAseq<sup>38</sup> largely overlapped our scRNA DEGs. Taken together, our identified enriched signaling pathways suggests that both TCR engagement and cytokine-induced JAK/STAT signaling are critically involved in the persistence and proliferation of CTCL cells in patients. In addition to the increase in several memory/activation markers (*SELL*, *CCR7*, *ITGBB1*, *BRD2*, *TNFRSF25*, *REL*, *TSPAN2*, *TNFRSF4*, and *NR4A2*) in CTCL, the DEG profile also revealed that exhausted immune marker genes (*TOX*, *TIGIT*, *CTLA4*, *PDCD1*, and *LAG3*) were significantly increased in CTCL cells, suggesting the possible influence of chronic antigen stimulation in patients with CTCL (Figure 4C).

In further considering the features of TCR activation and T-cell exhaustion that may affect the antiapoptotic and proliferative behavior of CTCL cells, we established an in vitro culture system to assess the relevance of TCR engagement by using anti-CD3/anti-CD28 stimulation, with and without resting the cells before stimulation, given that prior studies have shown that exhausted T cells proliferate again after withdrawal of chronic antigen stimulation.<sup>39,40</sup> We postulated that adding a resting period for patient-derived CTCL cells before TCR restimulation would promote their proliferation ex vivo. Indeed, CTCL cells minimally proliferated without TCR engagement, yet did so much more readily under conditions of a 4-day period of rest before TCR activation (Figure 4D-E; supplemental Figures 6 and 7), suggesting that malignant CTCL cells have the capacity to proliferate in a TCR-dependent manner. We also confirmed, in the CTCL cells of our samples, the upregulation of previously identified *CCR4* and *KIR3DL2* (Figure 4C), both of which are current therapeutic targets.<sup>41-43</sup> In addition, we found that expression of *CD82*, another gene encoding a cell surface protein, was significantly upregulated, suggesting its potential as a novel therapeutic target. DEG analysis was also performed to compare CTCLs from 2 different diagnosis categories, MF and SS, the latter of which carries a worse prognosis.<sup>44</sup> We found that 7 genes were upregulated, whereas 28 genes were downregulated in SS relative to MF, suggesting that these are potential biomarkers for diagnosis and prognosis and requiring further investigation (supplemental Figure 8).

## CD82 regulates CTCL proliferation and apoptosis through the JAK/STAT and AKT/PI3K pathways

We further characterized our newly identified CTCL DEG *CD82* in scRNAseq data and found that this surface protein, like *CCR4* and *KIR3DL2*, is intermediately expressed in the putative transitional CD4<sup>+</sup> T-cell population, and at a much lower level in normal CD4<sup>+</sup> T cells (Figure 5A). Furthermore, flow cytometry confirmed that the level of cell surface CD82 protein expression by CTCL cells was significantly higher than in normal CD4<sup>+</sup> T cells from the same patients (Figure 5B; supplemental Figure 9). To understand the function of CD82 in CTCL cells, we used CRISPR-Cas9 to knock out the *CD82* gene in isolated patient CTCL cells, confirming the deletion at both the protein and mRNA levels (Figure 5C-D; supplemental Figure 10). We found that CD82 deficiency markedly reduced the proliferative capacity of the activated CTCL cells (Figure 5E-F) and that apoptotic cells largely increased within the CD82-knockout CTCL cultures (Figure 5G). Taken together, features of CD82 expression, along with their relevance to CTCL cell proliferation and survival, suggest a therapeutic targeting strategy that could facilitate the elimination of CD82-expressing circulating T cells and/or blocking CD82-dependent CTCL-cell proliferation and increasing apoptosis. Notably, other studies have shown that CD82 promotes the survival of AML cells through JAK/STAT and AKT/PI3K pathways.<sup>32,45</sup> Through phosphoprotein analysis of CD82 signaling pathway components via flow cytometry, we found reduced activation of JAK, STAT, and AKT in CD82-deficient CTCL cells, suggesting that CD82 also drives proliferation of CTCL cells via JAK/STAT and AKT signaling pathways (Figure 5H).

Our current enrichment analysis (Figure 4B) highlighted JAK/STAT activation pathways in CTCL cells, and our recent research helped elucidate the potential therapeutic role of the JAK-inhibitor ruxolitinib.<sup>17</sup> Although these data suggest that targeting JAK signaling has a potential role in the treatment of CTCL, we considered whether other JAK inhibitors would show enhanced activity across patients. Thus, we performed dose-response assays against a panel of agents exhibiting different JAK family member selectivity profiles, to identify their relative potential in the treatment of CTCL (Figure 5I). Of 13 assessed agents, pacritinib, fedratinib, and entrectinib displayed the greatest potency, with all patient samples showing a 50% inhibitory concentration of <10  $\mu$ M.

## Discussion

Unlike other hematopoietic malignancies that may have signature gene fusions or limited gene copy number alterations, the genetic landscape of CTCL is notably diffuse. The extensive variability of SCNVs and SSNVs that are present within CTCL cells challenges our understanding of CTCL etiology and pathogenesis in the development of therapeutics. Previously, we and others have used

**Figure 3. Multidimensional characterization of the intermediate cell population in CTCL.** (A) Three annotated groups of cells from each single-patient analysis are shown on the UMAP plot resulting from integration of the transcriptomes of 11 patients. DEGs among the 3 groups are presented in a heat map. (B) Bar plot displaying the composition of SSNVs (identified via CellSNP) of the intermediate and CTCL groups of a representative patient. SSNVs found in the normal CD4<sup>+</sup> T-cell population were considered to be individual-specific normal variants (Normal SNV [Background]). Common SSNVs are those mutations found in both the intermediate and CTCL cell populations. (C) Representative inferred SCNV map (identified via InferCNV). (D) Landscape of inferred SCNVs among 10 patients with CTCL. (E) The composition of SCNVs (identified via InferCNV) of the intermediate and CTCL groups. (F) PHATE plot of a single patient with the SCNV level of each cell highlighted. (G) The significantly different level of SCNVs between the intermediate and CTCL cell groups (unpaired  $t$  test,  $\sim 10$  000 cells).

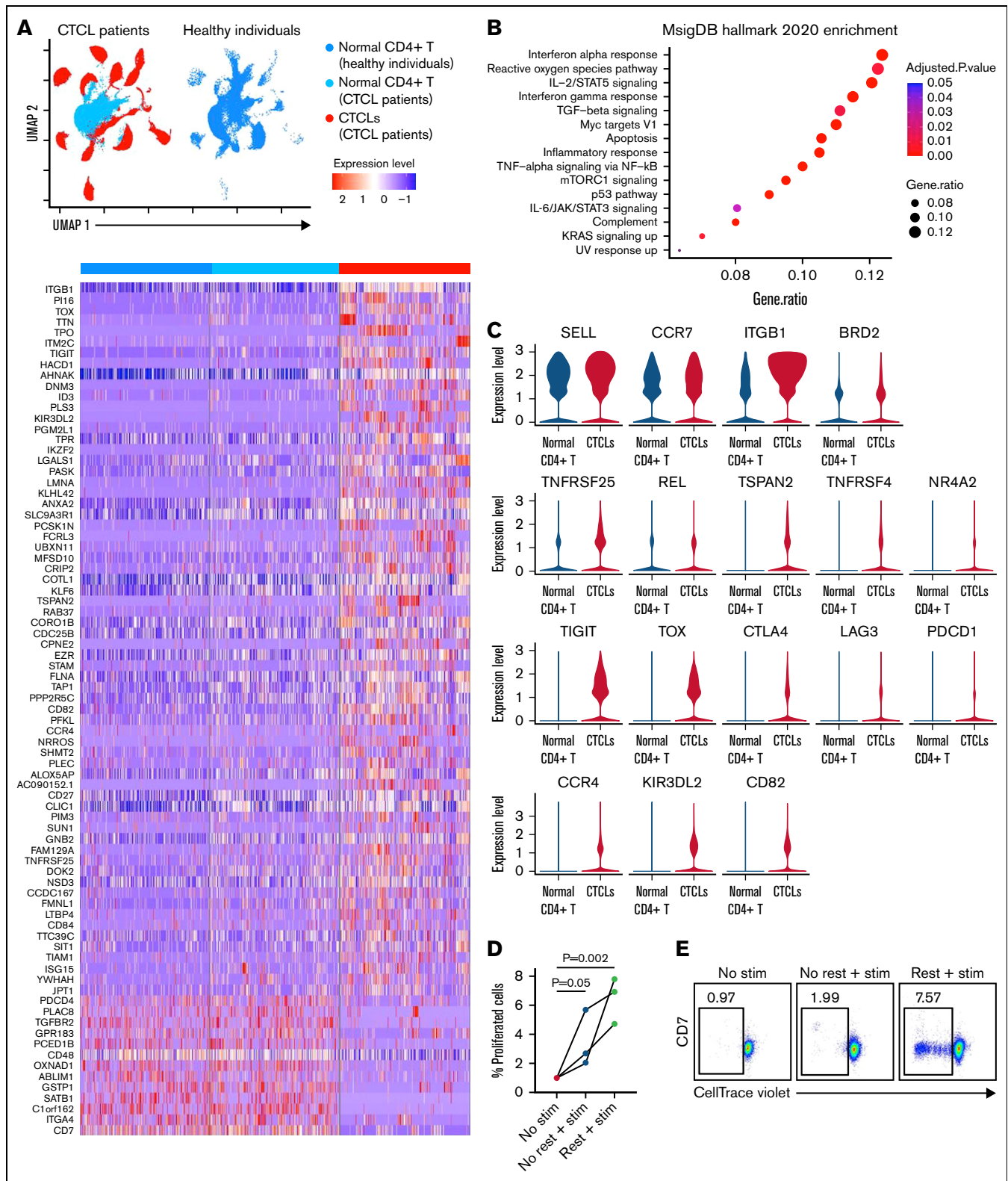


**Figure 4. Transcriptional characteristics of common features among heterogeneous patients with CTCL.** (A) Side-by-side view of the integrated UMAP of CD4<sup>+</sup> T cells from 11 patients with CTCL and 3 healthy controls, along with a heat map displaying the DEGs when all CTCLs cells were compared with all normal CD4<sup>+</sup> T cells combined from patients and healthy controls (heat map: minimum percentage >0.25%, minimum difference in percentages >0.2; adjusted  $P \leq .05$ , log fold change threshold = 0.25). (B) Pathway analysis of all DEGs revealed 15 enriched (adjusted  $P \leq .05$ ) pathways in the CTCLs. (C) Plots demonstrate increased expression of the central memory T-cell activation genes *SELL*, *CCR7*, *ITGB1*, *BRD2*, *TNFRSF25*, *REL*, *TSPAN2*, *TNFRSF4*, and *NR4A2* and the T-cell exhaustion genes *TIGIT*, *TOX*, *CTLA4*, *LAG3*, and *PDCD1* in CTCLs

bulk genetic and expression analyses to address these challenges. More recently, Herrera et al<sup>12</sup> and Borchering et al<sup>11</sup> combined RNAseq with TCRseq and showed the heterogeneity of CTCL cells, which reflects differential disease development stages, treatment sensitivities, and tissue microenvironment localization. By also using an integrative analysis combining scRNAseq and scTCRseq with PHATE analysis, we were able to provide novel insights into the development and progression of CTCL and to identify promising therapeutic strategies.

The propensity for a Th2 phenotype, known to drive symptomatic features of CTCL, or a Treg phenotype among CTCL cells is also a likely contributor to the decreased cellular immunity in patients with CTCL that is evidenced by an increased risk of herpes zoster and secondary malignancies.<sup>15,46</sup> Specific cytokines play critical roles in the pathogenesis of Th2-like CTCL cells. Interleukin-4 (IL-4) induces the differentiation of naive Th to the Th2 phenotype, which subsequently produces additional IL-4 in a positive feedback loop. In addition, Th2 effector cytokines IL-5, IL-13, and IL-31 are overexpressed in CTCL cells.<sup>47-49</sup> IL-5 is responsible for the maturation and activation of eosinophils and, together with IL-13, promotes allergic inflammation, whereas IL-31 is directly linked to pruritus in patients with CTCL.

Unlike bulk RNAseq, which usually requires sorting of CTCL cells based on loss of T-cell markers such as CD7 and CD26, which are not always consistent, our parallel scRNAseq and scTCRseq sequencing accurately identified malignant cells via the annotation of the dominant monoclonal TCR sequence onto the subgroup of cells generated by unbiased clustering. The PHATE algorithm further generated cell trajectories that reflected the developmental direction between different clusters. At single-cell resolution, our integrative analysis combined with PHATE consistently identified a transitional group of cells with a developmental stage between normal T cells and established malignant CTCL cells, which would not have been possible by bulk RNAseq. Our subsequent mutational analysis further supports a pathoetiology of CTCL that involves a progressive increase in mutation acquisition from normal T cells, to intermediate precancerous T cells, to the eventual emergence of bona fide malignant CTCL cells.

By comparing genetic mutations between the latter 2 groups, we further narrowed down a proportion of CTCL-unique mutations that may play pivotal roles in driving malignant transformation. In addition, given that the transcriptional and mutational profiles of the putative premalignant populations are intermediate between normal and malignant CD4 T cells, it is highly possible that there is a common genetic trajectory across different patients. Distinguishing such would require an additional genomic component to a future multiomics analysis of CTCL cells. Nonetheless, we used the program CellSNP<sup>34</sup> to determine the top 10 mutated genes (SSNVs in DNMT3, CCDC47, AC016831.7, RPTOR, TOX, SMYD3, SKAP1, TSHZ2, HCG27, MUC20-OT1) in our CTCL intermediate cells that were commonly shared (50% or greater

among our patient samples (supplemental Table 2). If such intermediate cells play a role in the development, maintenance, and/or transition into CTCL cells, tracking them before and after treatment may show whether their continued presence (or elimination) is associated with durability of response and disease recurrence.

That CTCL cells also show features of chronic activation and exhaustion led us to consider whether chronic antigen exposure is ongoing within patients with CTCL and whether it influences survival and proliferative advantages over acquired mutations. Indeed, despite the identification of SSNVs and SCNVs in cell cycle regulating tumor suppressor genes, such as *TP53* and *CDKN2A*, and T-cell activating genes, such as *STAT3* and *STAT5B*, CTCL cells are notoriously limited in their capacity to grow *ex vivo*. Again, this limitation is suggestive of a continued reliance on cognate antigen stimulation. The potential for dependence of CTCL on chronic antigen stimulation has also been supported by the clustering of CTCL around Langerhans cells in Pautrier's microabscesses<sup>1</sup> and around dendritic cells in *ex vivo* culture systems.<sup>50</sup> Thus, future improved screening and accurate identification of CTCL TCR specificity may provide additional insight into development of CTCL.

Postthymically, T-cell cycling is normally regulated, first by the differentiation of naive T cells into effector and memory T cells after initial exposure to cognate antigenic peptides along with costimulatory signals (eg, via CD28). Second, repetitive antigen exposures thereafter may further drive effector/memory T-cell clonal expansion, whereas chronic exposure may trigger an exhaustive state characterized by unresponsiveness to antigen stimulation and increased expression of coinhibitory molecules. CTCL cells show features of both a chronic activation and chronic exhaustion state that may lead to perpetuation of low-level proliferation of CTCL precursor cells. How and when such cells acquire mutations is akin to similar questions for other premalignant states, including in epithelial malignancies (eg, cervical intraepithelial neoplasia/cervical cancer, and actinic keratosis/skin) and hemopoietic cancers (eg, myelodysplastic syndrome/AML and circulating monoclonal B-cell lymphoproliferative states/B-cell leukemias in the bone marrow and blood).

Analysis of DEGs revealed TCR-induced T-cell activation and exhaustion markers in CTCLs, and we demonstrated that the induction of optimized CTCL cell proliferation requires short-term rest to recover from the exhaustive state, followed by TCR stimulation, which suggests a possible *in vivo* CTCL dynamic. The skin or skin-draining lymphoid organs may provide an antigen-dependent CTCL stimulatory microenvironment to continuously drive their proliferation. Although chronic antigen presentation may shift activated CTCL cells to a more exhausted state, we postulate that this can be reversed by egressing into blood circulation where the absence of antigen provides a resting condition for the CTCL cells, until they migrate back to the skin and/or lymph nodes for another round of stimulation and proliferation.

**Figure 4 (continued)** vs normal CD4<sup>+</sup> T cells, as well as increased *CD82*, *CCR4*, and *KIR3DL2* gene expression in CTCLs. (D) The percentage of CTCLs that proliferate in response to TCR engagement was significantly increased after a period of rest *in vitro*. Each line represents 1 patient-derived sample (n = 3). (E) Representative flow cytometric analysis of the proliferative capacity of CTCL cells. Cells were cultured with no stimulation for 4 days (No Stim) or were stimulated immediately after isolation (No Rest + Stim) or after a 4-day rest (Rest+Stim). Stimulation consisted of anti-CD3+anti-CD28 for 2 days followed by washing and a 2-day expansion in the absence of stimuli. UMAP, Uniform Manifold Approximation and Projection.

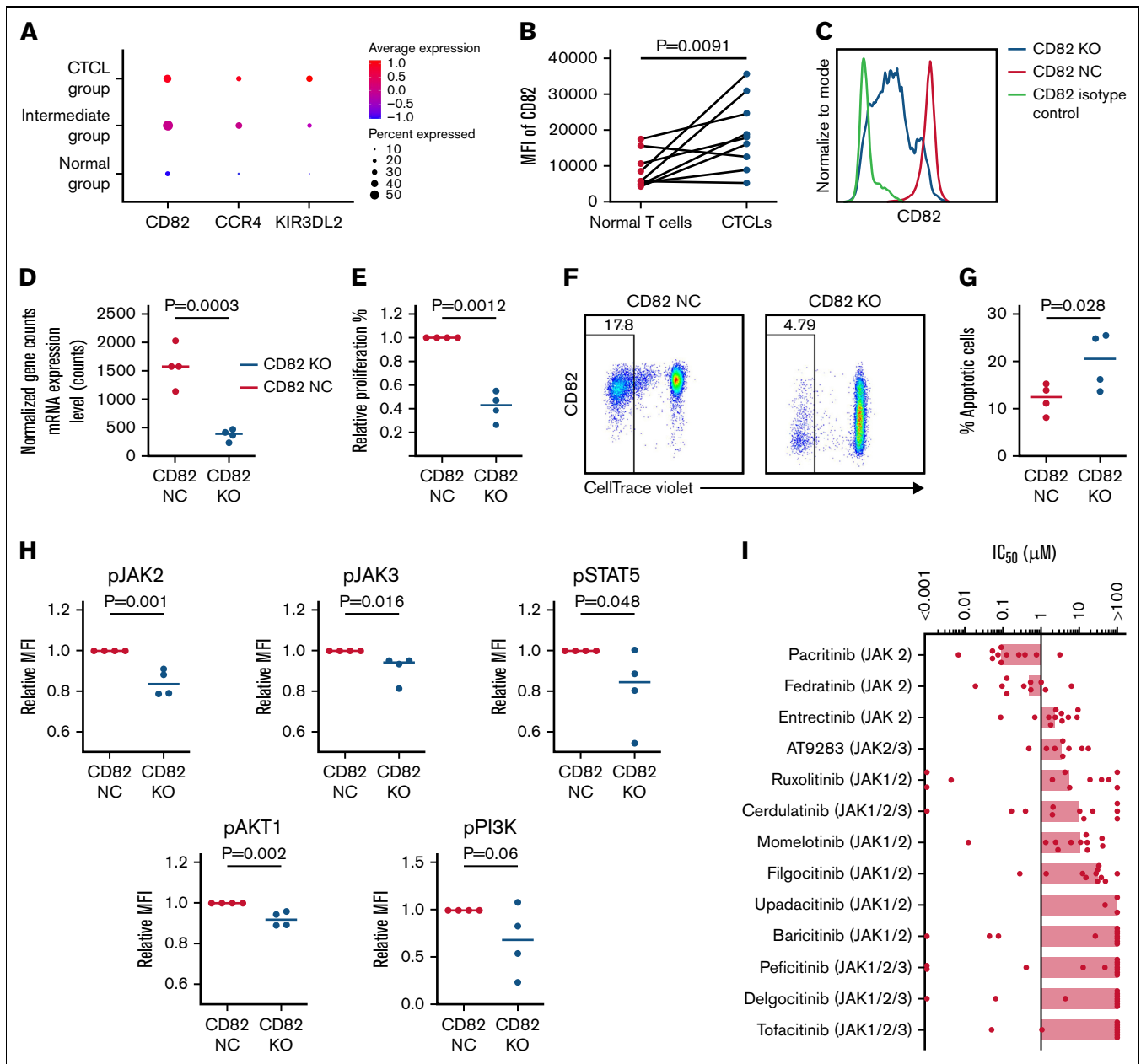


**Figure 5. CTCL hallmark gene *CD82* regulates proliferation and apoptosis via the JAK-STAT signaling pathway.** (A) Genes *CD82*, *CCR4*, and *KIR3DL2* displayed a similar monotonical expression pattern increasing from normal to intermediate to CTCL groups. (B) Mean fluorescence intensity (MFI) of *CD82* protein expression in  $CD4^+$  CTCL cells compared with normal  $CD4^+$  T cells from CTCL patient-derived PBMCs ( $n = 9$ ; 1-tailed  $t$  test). (C) Representative histograms comparing *CD82* expression in purified CTCL cells that have undergone either *CD82* knockout (*CD82*-KO, blue) or mock knockout (*CD82*-NC [negative control], red). (D) Bulk RNAseq was used to confirm *CD82* expression in purified CTCL cells before and after *CD82* knockout. (E) Comparison of the relative percentage of CTCL cell proliferation in *CD82* knockout and mock knockout CTCLs ( $n = 4$ ; 1-tailed paired  $t$  test). (F) Representative flow cytometric analysis of the proliferative capacity of CTCL cells (*CD82*-KO and *CD82*-NC) cultured for 2 days after anti-*CD3*+anti-*CD28* stimulation for 2 days. (G) Comparison of the percentage of apoptotic cells present in *CD82* knockout and mock knockout CTCLs in the proliferation experiment in panel E. (H) Comparison of the relative level of phosphorylation of JAK2, JAK3, STAT5, AKT1, and PI3K in activated and proliferated CTCL cells after *CD82* knockout or mock knockout cells cultured for 2 days after anti-*CD3*+anti-*CD28* stimulation for 2 days. (I) CTCL cells isolated from patient peripheral blood were incubated for 72 hours with a range of concentrations of various JAK inhibitors, from which the 50% inhibitory concentrations were calculated. Each dot represents a single patient's response to a single drug.

Our biomics analysis also suggested 2 novel therapeutic strategies for CTCL. We identified the overexpressed cell surface marker *CD82* and showed that *CD82* knockout reduced CTCL cell proliferation and increased apoptosis. In addition, reduced activation

of downstream JAK, STAT, and AKT were seen in *CD82*-deficient CTCL cells. Given that *CD82* expression is not limited to CTCL cells,<sup>51,52</sup> emerging strategies (eg, bispecific antibodies and/or prodrug-enzyme-paired agents) would be necessary to

therapeutically target this surface protein. Our investigation of the effect of specific JAK family member inhibition on patient-derived CTCL cell viability suggests certain JAK inhibitors may more effectively target CTCL cells across patients, but clinical studies are necessary to fully elucidate the safety and efficacy of such JAK inhibitors in the treatment of patients with CTCL.

## Acknowledgments

This work was supported by the R. S. Evans Foundation and the Cutaneous Lymphoma Foundation.

## Authorship

Contribution: J.R., J.M.L., X.L., A.L.O.K., F.N.M., S.X., and M.G. designed the experiments; M.G., F.M.F., and K.R.C. obtained informed consent and samples from the patients; J.R., A.L.O.K., F.N.M., and S.X. performed the experiments; J.R., R.Q., N.-T.R.,

B.K.R., B.E., S.G., G.W., A.L.O.K., F.N.M., and S.X. analyzed the data; J.R., R.Q., N.-T.R., J.M.L., A.L.O.K., F.N.M., S.X., Y.H., W.D., Y.K., S.K., and M.G. participated in discussions of the data; J.R., R.Q., N.-T.R., J.M.L., and M.G. wrote the manuscript; and all authors reviewed and edited the manuscript.

Conflict-of-interest disclosure: The authors declare no competing financial interests.

ORCID profiles: R.Q., [0000-0002-8258-8287](#); N.-T.R., [0000-0002-8247-7165](#); Y.H., [0000-0001-6803-5195](#); B.E., [0000-0003-2069-4938](#); B.K.R., [0000-0001-9675-7718](#); S.X., [0000-0001-9389-8953](#); F.M.F., [0000-0001-7843-3162](#); Y.K., [0000-0002-3035-071X](#); M.G., [0000-0003-1887-9343](#).

Correspondence: Michael Girardi, Department of Dermatology, Yale University School of Medicine, 333 Cedar St, PO Box 208059, New Haven, CT 06520; email: [michael.girardi@yale.edu](mailto:michael.girardi@yale.edu).

## References

1. Girardi M, Heald PW, Wilson LD. The pathogenesis of mycosis fungoides. *N Engl J Med*. 2004;350(19):1978-1988.
2. Agar NS, Wedgeworth E, Crichton S, et al. Survival outcomes and prognostic factors in mycosis fungoides/Sézary syndrome: validation of the revised International Society for Cutaneous Lymphomas/European Organisation for Research and Treatment of Cancer staging proposal. *J Clin Oncol*. 2010;28(31):4730-4739.
3. Lin WM, Lewis JM, Filler RB, et al. Characterization of the DNA copy-number genome in the blood of cutaneous T-cell lymphoma patients. *J Invest Dermatol*. 2012;132(1):188-197.
4. Fischer TC, Gellrich S, Mucic JM, et al. Genomic aberrations and survival in cutaneous T cell lymphomas. *J Invest Dermatol*. 2004;122(3):579-586.
5. Choi J, Goh G, Walradt T, et al. Genomic landscape of cutaneous T cell lymphoma. *Nat Genet*. 2015;47(9):1011-1019.
6. Chang LW, Patrone CC, Yang W, et al. An integrated data resource for genomic analysis of cutaneous T-cell lymphoma. *J Invest Dermatol*. 2018;138(12):2681-2683.
7. McGirt LY, Jia P, Baerenwald DA, et al. Whole-genome sequencing reveals oncogenic mutations in mycosis fungoides. *Blood*. 2015;126(4):508-519.
8. da Silva Almeida AC, Abate F, Khiabani H, et al. The mutational landscape of cutaneous T cell lymphoma and Sézary syndrome. *Nat Genet*. 2015;47(12):1465-1470.
9. Ungewickell A, Bhaduri A, Rios E, et al. Genomic analysis of mycosis fungoides and Sézary syndrome identifies recurrent alterations in TNFR2. *Nat Genet*. 2015;47(9):1056-1060.
10. Iyer A, Hennessey D, O'Keefe S, et al. Clonotypic heterogeneity in cutaneous T-cell lymphoma (mycosis fungoides) revealed by comprehensive whole-exome sequencing. *Blood Adv*. 2019;3(7):1175-1184.
11. Borchering N, Voigt AP, Liu V, Link BK, Zhang W, Jabbari A. Single-cell profiling of cutaneous T-cell lymphoma reveals underlying heterogeneity associated with disease progression. *Clin Cancer Res*. 2019;25(10):2996-3005.
12. Herrera A, Cheng A, Mimitou EP, et al. Multimodal single-cell analysis of cutaneous T-cell lymphoma reveals distinct subclonal tissue-dependent signatures. *Blood*. 2021;138(16):1456-1464.
13. Gaydosik AM, Tabib T, Geskin LJ, et al. Single-cell lymphocyte heterogeneity in advanced cutaneous T-cell lymphoma skin tumors. *Clin Cancer Res*. 2019;25(14):4443-4454.
14. Bobrowicz M, Fassnacht C, Ignatova D, Chang YT, Dimitriou F, Guenova E. Pathogenesis and therapy of primary cutaneous T-cell lymphoma: Collegium Internationale Allergologicum (CIA) Update 2020. *Int Arch Allergy Immunol*. 2020;181(10):733-745.
15. Stolareno V, Namini MRJ, Hasselager SS, et al. Cellular interactions and inflammation in the pathogenesis of cutaneous T-cell lymphoma. *Front Cell Dev Biol*. 2020;8:851.
16. Dummer R, Vermeer MH, Scarisbrick JJ, et al. Cutaneous T cell lymphoma. *Nat Rev Dis Primers*. 2021;7(1):61.
17. Yumeen S, Mirza FN, Lewis JM, et al. JAK inhibition synergistically potentiates BCL2, BET, HDAC, and proteasome inhibition in advanced CTCL. *Blood Adv*. 2020;4(10):2213-2226.
18. Karagianni F, Piperi C, Mpakou V, et al. Ruxolitinib with resminostat exert synergistic antitumor effects in cutaneous T-cell lymphoma. *PLoS One*. 2021;16(3):e0248298.

19. Yumeen S, Girardi M. Insights Into the molecular and cellular underpinnings of cutaneous T cell lymphoma. *Yale J Biol Med.* 2020;93(1):111-121.
20. Ghazawi FM, Alghazawi N, Le M, et al. Environmental and other extrinsic risk factors contributing to the pathogenesis of cutaneous T cell lymphoma (CTCL). *Front Oncol.* 2019;9:300.
21. Chevret E, Andrique L, Prochazkova-Carlotti M, et al. Telomerase functions beyond telomere maintenance in primary cutaneous T-cell lymphoma. *Blood.* 2014;123(12):1850-1859.
22. Wu K, Lund M, Bang K, Thestrup-Pedersen K. Telomerase activity and telomere length in lymphocytes from patients with cutaneous T-cell lymphoma. *Cancer.* 1999;86(6):1056-1063.
23. Jones CL, Degasperi A, Grandi V, et al; Genomics England Research Consortium. Spectrum of mutational signatures in T-cell lymphoma reveals a key role for UV radiation in cutaneous T-cell lymphoma. *Sci Rep.* 2021;11(1):3962.
24. Brash DE. UV signature mutations. *Photochem Photobiol.* 2015;91(1):15-26.
25. Gibson JF, Huang J, Liu KJ, et al. Cutaneous T-cell lymphoma (CTCL): current practices in blood assessment and the utility of T-cell receptor (TCR)-V $\beta$  chain restriction. *J Am Acad Dermatol.* 2016;74(5):870-877.
26. Robins HS, Campregher PV, Srivastava SK, et al. Comprehensive assessment of T-cell receptor beta-chain diversity in alphabeta T cells. *Blood.* 2009;114(19):4099-4107.
27. Kirsch IR, Watanabe R, O'Malley JT, et al. TCR sequencing facilitates diagnosis and identifies mature T cells as the cell of origin in CTCL. *Sci Transl Med.* 2015;7(308):308ra158.
28. Gao JX. Cancer stem cells: the lessons from pre-cancerous stem cells. *J Cell Mol Med.* 2008;12(1):67-96.
29. Wacholder S. Precursors in cancer epidemiology: aligning definition and function. *Cancer Epidemiol Biomarkers Prev.* 2013;22(4):521-527.
30. Moon KR, van Dijk D, Wang Z, et al. Visualizing structure and transitions in high-dimensional biological data [published correction appears in *Nat Biotechnol.* 2020 Jan;38(1):108]. *Nat Biotechnol.* 2019;37(12):1482-1492.
31. Iwata S, Kobayashi H, Miyake-Nishijima R, et al. Distinctive signaling pathways through CD82 and beta1 integrins in human T cells. *Eur J Immunol.* 2002;32(5):1328-1337.
32. Nishioka C, Ikezoe T, Takeuchi A, Nobumoto A, Tsuda M, Yokoyama A. The novel function of CD82 and its impact on BCL2L12 via AKT/STAT5 signal pathway in acute myelogenous leukemia cells. *Leukemia.* 2015;29(12):2296-2306.
33. Lebel-Binay S, Lagaudri re C, Fradelizi D, Conjeaud H. CD82, member of the tetra-span-transmembrane protein family, is a costimulatory protein for T cell activation. *J Immunol.* 1995;155(1):101-110.
34. Huang X, Huang Y. Cellsnp-lite: an efficient tool for genotyping single cells. *Bioinformatics.* 2021;37(23):btab358.
35. Tickle TTI, Georgescu C, Brown M, Haas B. inferCNV of the Trinity CTAT Project. 2019. Accessed 21 October 2021. Available at: <https://github.com/broadinstitute/inferCNV>
36. Chen EY, Tan CM, Kou Y, et al. Enrichr: interactive and collaborative HTML5 gene list enrichment analysis tool. *BMC Bioinformatics.* 2013;14(1):128.
37. Xie Z, Bailey A, Kuleshov MV, et al. Gene set knowledge discovery with enrichr. *Curr Protoc.* 2021;1(3):e90.
38. Patil K, Kuttikrishnan S, Khan AQ, et al. Molecular pathogenesis of cutaneous T cell lymphoma: role of chemokines, cytokines, and dysregulated signaling pathways. *Semin Cancer Biol.* 2021;S1044-579X(21)00296-0.
39. Tonnerre P, Wolski D, Subudhi S, et al. Differentiation of exhausted CD8<sup>+</sup> T cells after termination of chronic antigen stimulation stops short of achieving functional T cell memory. *Nat Immunol.* 2021;22(8):1030-1041.
40. Abdel-Hakeem MS, Manne S, Beltra JC, et al. Epigenetic scarring of exhausted T cells hinders memory differentiation upon eliminating chronic antigenic stimulation. *Nat Immunol.* 2021;22(8):1008-1019.
41. Nicolay JP, Albrecht JD, Alberti-Violetti S, Berti E. CCR4 in cutaneous T-cell lymphoma: therapeutic targeting of a pathogenic driver. *Eur J Immunol.* 2021;51(7):1660-1671.
42. Gniadecki R. CCR4-targeted therapy in cutaneous T-cell lymphoma. *Lancet Oncol.* 2018;19(9):1140-1141.
43. Bagot M, Porcu P, Marie-Cardine A, et al. IPH4102, a first-in-class anti-KIR3DL2 monoclonal antibody, in patients with relapsed or refractory cutaneous T-cell lymphoma: an international, first-in-human, open-label, phase 1 trial. *Lancet Oncol.* 2019;20(8):1160-1170.
44. Olsen EA, Whittaker S, Kim YH, et al; Cutaneous Lymphoma Task Force of the European Organisation for Research and Treatment of Cancer. Clinical end points and response criteria in mycosis fungoides and S zary syndrome: a consensus statement of the International Society for Cutaneous Lymphomas, the United States Cutaneous Lymphoma Consortium, and the Cutaneous Lymphoma Task Force of the European Organisation for Research and Treatment of Cancer. *J Clin Oncol.* 2011;29(18):2598-2607.
45. Nishioka C, Ikezoe T, Yang J, et al. CD82 regulates STAT5/IL-10 and supports survival of acute myelogenous leukemia cells. *Int J Cancer.* 2014;134(1):55-64.
46. Lebas E, Arrese JE, Nikkels AF. Risk factors for skin infections in mycosis fungoides. *Dermatology.* 2016;232(6):731-737.
47. Nielsen M, Nissen MH, Gerwien J, et al. Spontaneous interleukin-5 production in cutaneous T-cell lymphoma lines is mediated by constitutively activated Stat3. *Blood.* 2002;99(3):973-977.
48. Geskin LJ, Viragova S, Stolz DB, Fuschiotti P. Interleukin-13 is overexpressed in cutaneous T-cell lymphoma cells and regulates their proliferation. *Blood.* 2015;125(18):2798-2805.

49. Cedeno-Laurent F, Singer EM, Wysocka M, et al. Improved pruritus correlates with lower levels of IL-31 in patients with CTCL under different therapeutic modalities. *Clin Immunol*. 2015;158(1):1-7.
50. Berger CL, Hanlon D, Kanada D, et al. The growth of cutaneous T-cell lymphoma is stimulated by immature dendritic cells. *Blood*. 2002;99(8):2929-2939.
51. Shibagaki N, Hanada K, Yamashita H, Shimada S, Hamada H. Overexpression of CD82 on human T cells enhances LFA-1 / ICAM-1-mediated cell-cell adhesion: functional association between CD82 and LFA-1 in T cell activation. *Eur J Immunol*. 1999;29(12):4081-4091.
52. Wei Q, Zhang F, Richardson MM, et al. CD82 restrains pathological angiogenesis by altering lipid raft clustering and CD44 trafficking in endothelial cells. *Circulation*. 2014;130(17):1493-1504.